J Fluoresc (2012) 22:961–970
DOI 10.1007/s10895-011-1034-9

ORIGINAL PAPER

Syntheses and pH Sensing Applications of Imine-Coupled Phenol and Polyphenol Species Derived from 2-Amino-4-Nitrophenol

Mehmet Yıldırım · Aysel Aydın · İsmet Kaya

Received: 21 October 2011 / Accepted: 28 December 2011 / Published online: 7 January 2012

Abstract Developing of new generation optical polymeric pH sensors has increasing importance due to their stable structures. Available polymeric sensors for different pH ranges are already needed. In the present study new kinds of monomeric and polymeric absorption pH sensors (HBANP and PHBANP) derived from 2-amino-4-nitrophenol were prepared. The novel sensors were investigated in various pH values using spectrophotometric, spectrofluorometric, and electrochemical techniques. The sensors showed sigmoidal correlations vs. pH range in optical measurements. These correlations were improved as mathematical formula to obtain the solution pH. HBANP and PHBANP differed from each other by response fields. HBANP had a sharp absorption increase between the pH of 6.5→7.5 while PHBANP spectrophotometrically responded at lower pHs. HBANP was colorless in acidic pHs, yellow-colored in neutral media and red-colored in alkaline pHs. With its colorimetric responses in various pHs HBANP can be used to develop color-tunable pH sensors. Electrochemical oxidation peak potentials and currents also particularly changed in various pHs.

Keywords Polyazomethine · pH sensor · Optical sensor · Fluorescence · Oligophenol · Cyclic voltammetry

Introduction

During the last few decades global research and development (R&D) on the field of sensors has exponentially expanded in terms of financial investment, the published literature, and the number of active researches [1–4]. Glass pH electrodes are unsuitable for certain applications like determination of intracellular pH, microscopy studies as well as measurement of extreme pH values (<1 or >9) [5]. New kinds of optical sensors have attracted great attention of researchers due to their possible applications in industrial, environmental, and medicinal areas [6, 7]. Several kinds of optical pH and ion sensors have been published so far [8–13]. Optical sensors have a lot of advantages including cheapness, fine sensitivity, freedom from electrical interference, safety, and being easy to apply [14]. In addition, a lot of analytes could be analyzed by optical sensors which cannot be detected by another method. Another advantage of pH sensors over pH electrodes is their wide pH scales. There are, however, only a few optical pH sensors being used at high or low pHs [14–19]. Developing available pH sensors in different pH ranges is still needed. Moreover, polymeric based pH sensors have been prepared by using electrical conductive polyaniline [20], polypyrrole [21] etc. Hydrogel-based pH sensors using mechano-electrical transducers have been developed depending on swelling characteristics those change by pH changing [22, 23]. Potentiometric methods have been also employed to develop new pH sensors as well as optical and fluorescence measurements [24]. pH dependence of electrochemical oxidation peak potential and/or current could be used in potentiometric sensors [25].

Polyazomethines (PAMs) have been employed in many fields with their useful properties. Several kinds of PAMs and their oligophenol derivatives with polyconjugated structures have been found as semi-conductive materials [26, 27]. In the present study we aimed to obtain new kind of PAMs and the monomeric Schiff base model having pH sensitivity properties. The novel pH sensors were synthesized using 2-amino-4-nitrophenol. Optical, electrochemical, and fluorescence responses of the new sensors were investigated. The results

M. Yıldırım · A. Aydın · İ. Kaya (✉)
Faculty of Sciences and Arts, Department of Chemistry,
Çanakkale Onsekiz Mart University,
TR-17020 Çanakkale, Turkey
e-mail: kayaismet@hotmail.com

showed that the Schiff base and its polymer work in different pH ranges. The sensing mechanism of the novel sensors was also suggested to clarify the different available pH ranges of the monomer and polymer.

Experimental

Materials

4-hydroxybenzaldehyde (4-HBA), 2-amino-4-nitrophenol (ANP), methanol, ethanol, acetone, dioxane, ethyl acetate, toluene, n-hexane, dichloromethane, $CHCl_3$, THF, DMF were supplied by Merck Chemical Co. and used as received. 30% aqueous solution of sodium hypo chlorite (NaOCl) was supplied from Paksoy Chemical Co. (Turkey).

Preparation of the Materials

The Schiff base monomer, 2-(4-hydroxybenzylideneamino)-4-nitrophenol (HBANP), was prepared by the condensation reaction of 4-hydroxybenzaldehyde (3.66×10^{-4} kg, 3×10^{-3} mol) with 2-amino-4-nitrophenol (4.62×10^{-4} kg, 3×10^{-3} mol) in methanol (5×10^{-2} dm^3) achieved by boiling the mixture under reflux for 5 h. The precipitated Schiff base was filtered, recrystallized from methanol and dried in a vacuum desiccator (yield: 75%). Oxidative polycondensation (OP) product of HBANP, poly-2-(4-hydroxybenzylideneamino)-4-nitrophenol (PHBANP) was synthesized as follows: 2.58×10^{-4} kg of HBANP was dissolved in THF (1.5×10^{-2} dm^3) and placed into a 50 cm^3 three-necked round-bottom flask which was fitted with a condenser, stirrer, and an addition funnel containing 0.5 cm^3 of NaOCl aqueous solution (30% by weight). After heating up to 70 °C, NaOCl was added drop by drop over about 20 min. Reaction was maintained for 2 h under reflux. Then, the solvent was removed by evaporator. The product was washed with hot water (3×25 cm^3) and methanol (2×20 cm^3) to separate the mineral salts and unreacted monomers, respectively. The obtained polymer was dried in a vacuum oven at 60 °C for 24 h (yield: 62%) [28]. The reaction steps are given in Scheme 1. Aqueous organic solvents had been previously used in OP reactions of phenolic monomers with enzyme catalysts [29, 30].

Characterization Techniques

The solubility tests were carried out by using 1×10^{-6} kg sample and 1×10^{-3} dm^3 solvent at 25 °C. The infrared spectra were measured by Perkin Elmer Spectrum One FT-IR system using universal ATR sampling accessory within the wavenumbers of 4,000–650 cm^{-1}. The synthesized compounds were also characterized by ^{1}H- and ^{13}C-NMR spectra (Bruker AC FT-NMR spectrometer operating at 400 and 100.6 MHz, respectively) obtained in DMSO-d_6 as the solvent at 25 °C. Tetramethylsilane was used as internal standard. The number average molecular weight (M_n), weight average molecular weight (M_w) and polydispersity index (PDI) were determined by size exclusion chromatography (SEC) techniques of Shimadzu Co. For SEC investigations, an SGX (100 Å and 7 nm diameter loading material) 3.3 mm i.d. × 300 mm columns was used; eluent: DMF (0.4 ml/min), polystyrene standards were used. A refractive index detector (RID) and a UV detector were used to analyze the products at 25 °C.

Optical and Fluorescence Measurements

Fluorescence and absorption spectra were recorded by Shimadzu RF-5301PC spectrofluorophotometer and Perkin Elmer Lambda 25, respectively. Concentrations of the sensing materials (HBANP or PHBANP) in all optical measurements were

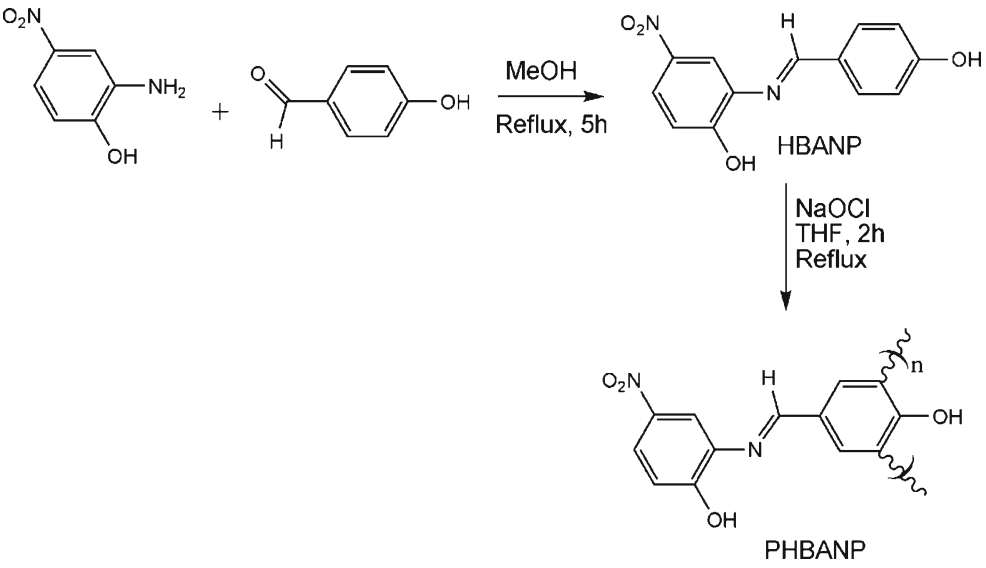

Scheme 1 Syntheses of the materials

5×10^{-5} kg L^{-1}. Measurements were carried out in methanol-water (1/2, v/v) solutions in the pH range of 2–10. pHs of the alkaline solutions (pH: 6–10) were adjusted by 0.1 mol dm^{-3} concentrated buffer solutions of Na_2HPO_4-NaH_2PO_4. The buffers with lower pHs (pH: 2–6) were prepared by 0.5 mol dm^{-3} HCl addition (different amounts for each solution) into the buffer with pH=6. UV–vis measurements were carried out in the wavelength range of 250–700 nm. Fluorescence measurements of HBANP were made in the range of 250–550 nm. Excitation wavelength for emission measurements and emission wavelength for excitation measurements were 260 and 523 nm, respectively.

Electrochemical Behaviours

Cyclic voltammetry (CV) measurements were carried out with a CHI 660 C Electrochemical Analyzer (CH Instruments, Texas, USA) at different pHs ranging from 3 up to 10. Various potential scan rates between 25 and 1,000 mV/s were used. All the experiments were performed in a dry box filled with argon at room temperature. The system consisted of a CV cell containing glassy carbon as the working electrode, platinum wire as the counter electrode, and Ag wire as the reference electrode. The voltammetric measurements of HBANP and PHBANP were carried out in methanol/buffer mixtures (1/4, v/v) and DMSO/buffer mixtures (1/4, v/v), respectively, each of which included 1×10^{-3} kg L^{-1} sample. Na_2HPO_4-NaH_2PO_4 salt mixture in the buffer solutions also acted as the supporting electrolyte.

Results and Discussion

Solubilities and Structures of the Compounds

HBANP has red colored-powder form and its polyphenol derivative, PEAPINP, is black colored. HBANP is completely soluble in many organic solvents such as methanol, acetone, THF, DMF, dichloromethane, and $CHCl_3$. However it's partially soluble in ethanol, n-hexane, toluene, ethyl acetate, and dioxane. PHBANP is completely soluble in THF, DMF, DMSO, and H_2SO_4 while it's partially soluble in methanol, ethanol, acetone, dichloromethane, $CHCl_3$, and ethyl acetate. Also it is insoluble in apolar solvents like n-hexane and toluene.

The FT-IR spectra of the reactives and the synthesized materials are given in Fig. 1. According to the obtained

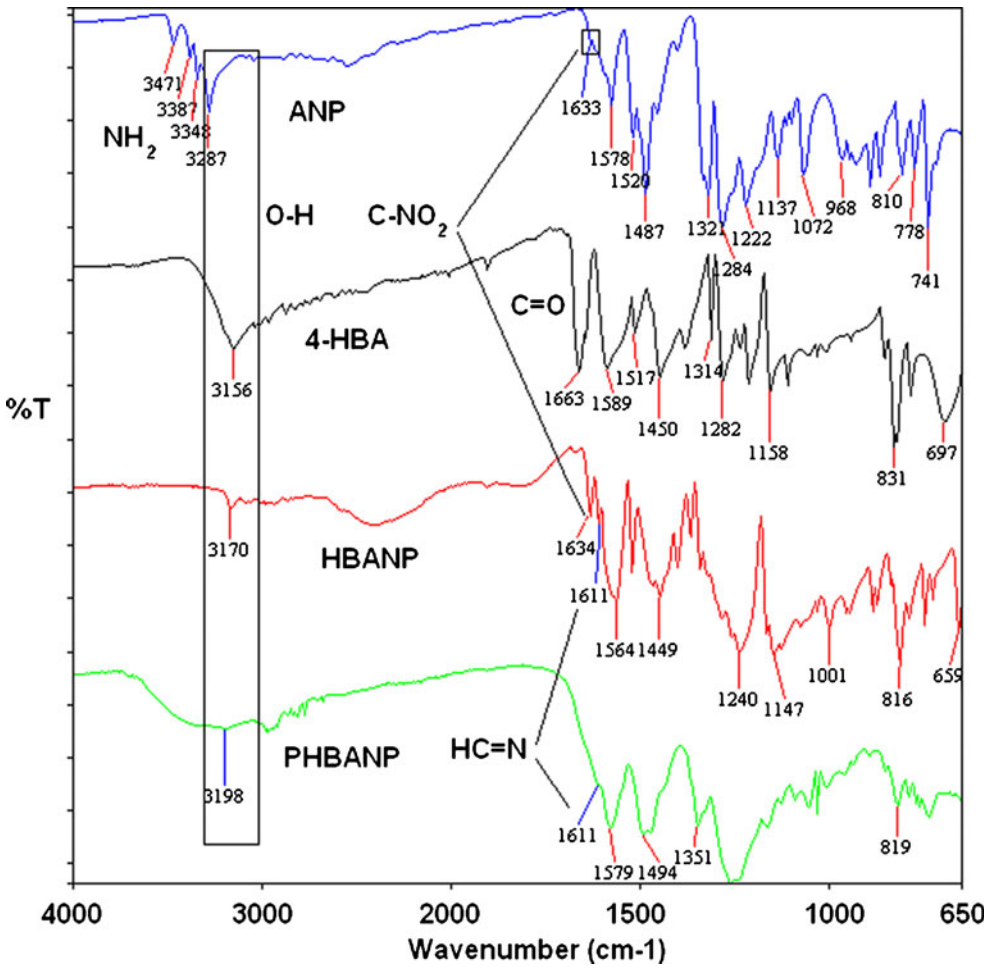

Fig. 1 FT-IR spectra of ANP, 4-HBA, and the synthesized materials

spectra the structure of HBANP is confirmed by disappearing of the C = O stretching of 4-HBA at 1,663 cm^{-1} and N-H stretch vibrations of ANP at 3,471, 3,387, and 3,348 cm^{-1}. Also, a new growing peak at 1,611 cm^{-1} indicating the formed imine bond stretching (HC = N) supports the Schiff base structure. In addition, widespread peaks are observed at the spectrum of PHBANP due to the polyconjugated structure [28]. HC = N stretch vibration of PHBANP is also observed at 1,611 cm^{-1}. After the polycondensation reaction O-H and C = C (aromatic) stretch vibrations shift to higher wavelengths from 3,170 to 3,198 cm^{-1} and from 1,564 to 1,579 cm^{-1}, respectively. The wide O-H band of PHBANP could be attributed to the intra-chain hydrogen bonding. C-NO_2 stretching vibration is also observed at 1,633–1,634 cm^{-1} at the spectra of ANP and HBANP [31].

The NMR analyses results of the synthesized compounds are given below. The ^{1}H and ^{13}C-NMR spectra of HBANP are shown in Fig. 2. According to Fig. 2a the structure of HBANP is confirmed by two -OH resonance signals at 10.64 and 9.81 ppm as well as imine (CH = N) peak at 8.67 ppm. The absence of -NH_2 and carbonyl (HC = O) peaks at the ^{1}H-NMR spectrum of HBANP indicates that the reaction was successfully carried out. As seen in the ^{13}C-NMR spectrum of HBANP C9 and C10 carbons have higher intensities than the others due to their higher numbers. ^{1}H-NMR spectrum of PHBANP is also given in Fig. 3. The assignments and the integrated areas of all peaks are shown on the spectrum. The radicalic polymerization mechanism of polyphenols has been previously investigated and presented in the literature [28]. This mechanism suggests that phenol-based monomers can be polymerized by C-C and C-O-C coupling of monomer units. The C-C coupling mechanism proceeds by intermolecular combination of the monomer units at the *ortho* and *para* positions of phenolic -OH. However, C-O-C coupling occurs by combination of a phenoxy radical with an *ortho* or *para* position of another monomer unit. Coupling selectivity of a corresponding monomer could be determined by comparison of the integrated areas of -OH and imine (HC = N) proton signals [28]. To determine the C-O-C coupling ratios of two -OH groups of HBANP the peak integrations are used. -OH peak integrations are lower than that of the imine proton. According

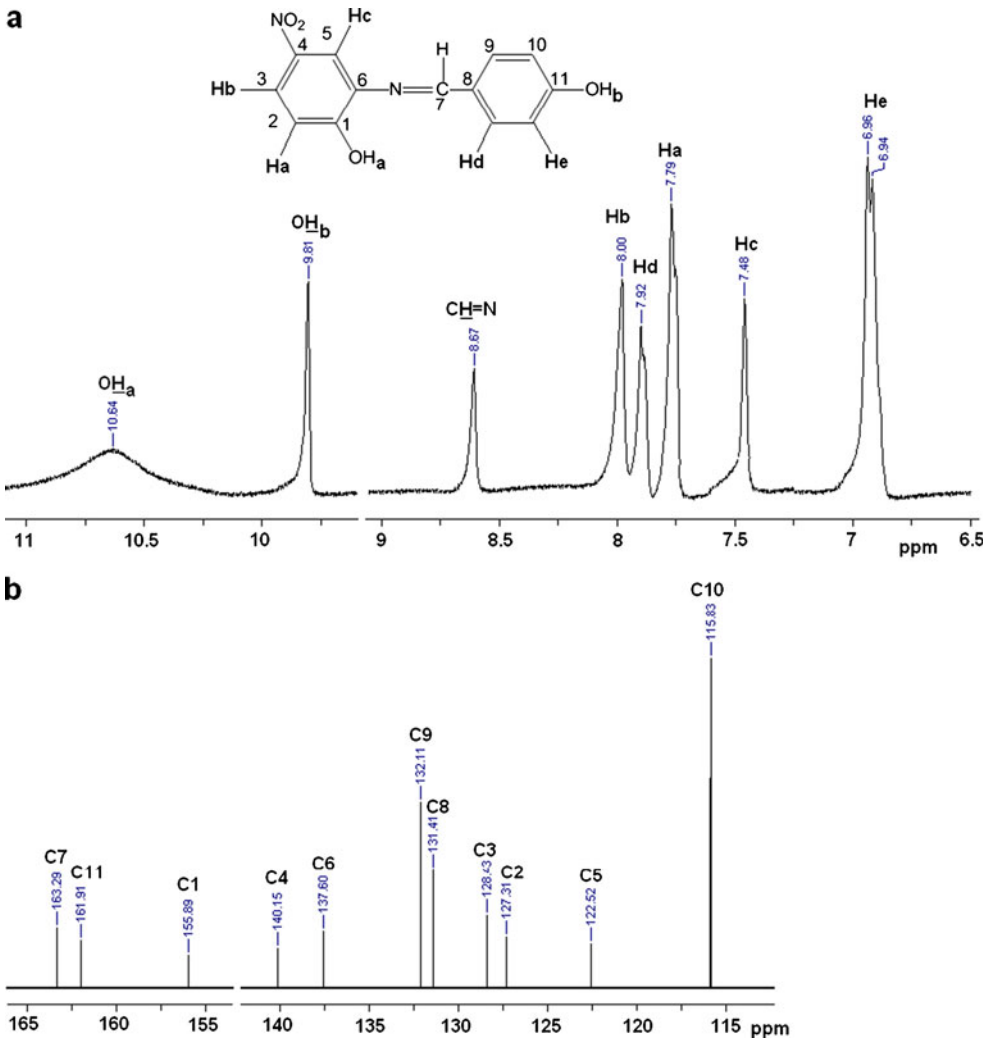

Fig. 2 ^{1}H-NMR (**a**) and ^{13}C-NMR spectra of HBANP

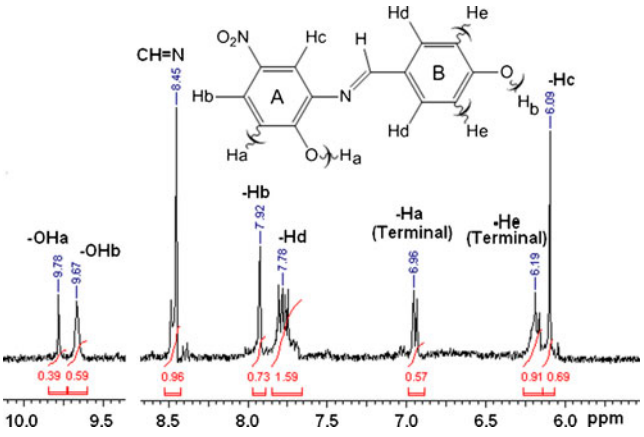

Fig. 3 ^{1}H-NMR spectrum of PHBANP

to the calculated integrations C-O-C coupling ratio of -OHa group (ring A) is nearly 60% and -OHb group of ring B is nearly 40%. A double peak at 6.96 ppm is assigned to terminal -Ha proton whose integration is relatively lower. However, the integration of -Ha is still high showing approximately 40% C-C ratio for the ring A. In addition, -He signal for the terminal units is observed at 6.19 ppm with the integration values of 0.91 indicating nearly 50% C-C coupling for the ring B. The obtained results clearly show that the OP reaction of HBANP proceeds by both coupling mechanisms and, resultantly, a decrease in phenolic -OH number is occurred.

HBANP: ^{1}H-NMR (DMSO): δ ppm, 10.64 (s, 1H, -OHa), 9.81 (s, 1H, -OHb), 8.67 (s, 1H, -CH = N-), 7.79 (d, 1H, Ar-Ha), 8.00 (d, 1H, Ar-Hb), 7.48 (s, 1H, Ar-Hc), 7.92 (d, 1H, Ar-Hd), 6.95 (d, 1H, Ar-He). ^{13}C-NMR (DMSO): δ ppm, 163.29 (C7-H), 161.91 (C11-ipso), 155.89 (C1-ipso), 140.15 (C4-ipso), 137.60 (C6-ipso), 132.11 (C9-H), 131.41 (C8-ipso), 128.43 (C3-H), 127.31 (C2-H), 122.52 (C5-H), 115.83 (C10-H).

PHBANP: ^{1}H-NMR (DMSO): δ ppm, 9.78 (s, -OHa), 9.67 (s, -OHb), 8.45 (s, -CH = N-), 7.92 (s, Ar-Hb), 7.78 (m, Ar-Hd), 6.96 (d, Ar-Ha (terminal)), 6.19 (d, Ar-He (terminal)), 6.09 (s, Ar-Hc).

According to the SEC chromatograms PHBANP has a single fraction. The number-average molecular weight (M_n), weight average molecular weight (M_w), and polydispersity index (*PDI*) values obtained from both RI and UV detectors are 26,250, 32,500 g mol^{-1}, and 1.238; and 24,450, 29,900 g mol^{-1}, and 1.222, respectively. According to these results PHBANP contains approximately 100–120 repeated units. The obtained molecular weights are relatively higher than the previously published azomethine linked oligophenol kinds. This could be attributed to the presence of more than one active phenolic group in the monomer compound which supplies several radical forms and possible coupling kinds [32].

Optical Measurements

Nitro (NO_2) and hydroxyl (-OH) substituents of HBANP and PHBANP are the corresponding sites from stable spectral changes depending on the pH values. According to the Huckel Calculation the charge densities of the oxygen atoms of -NO_2 are quite higher than those of the other oxygen and nitrogen atoms. This means that the protonation of HBANP occurs on -NO_2 oxygens in acidic conditions. This causes decreasing in conjugation of the molecule and inhibition of the photoinduced electron transfer (PET) between the electro-donor phenolic -OH and electro-acceptor -NO_2 groups (Scheme 2) [33, 34]. Moreover, two phenolic -OH protons behave as acidic protons in basic conditions and remove from the molecule at high pHs. As a result of the deprotonation in basic conditions, the formed phenoxy anions increase the electron density of the phenylene rings and the molecular conjugation. The increasing conjugation of HBANP from low to high pHs causes the colour change from colourless state to orange as well as red shift in the absorption edge. The color changes of HBANP between pH:3–10 are shown on the top of Fig. 4. The synthesized materials, then, can be used as color-tunable pH sensors due to the obtained color changes. Some other Schiff base derivatives have been also synthesized as colorimetric sensors in presence of different ions like fluoride [35].

The normalized absorption spectra of HBANP in different pH values are given in Fig. 4. The normalization process was made in the range of 250–300 nm. The peak in this region is due to the aromatic $\pi\rightarrow\pi^*$ transition and not affected by pH change as the absorption intensity. However, its absorption intensity is affected by concentration changes even if it is a very little change. To eliminate the effect of possible trace concentration variations on the optical measurements the normalization was carried out in the mentioned wavelength range. As seen in Fig. 4 the absorption increases with increasing pH are observed in two different regions whose peak values are 335 and 440 nm. The absorptions at 440 nm (A_{440}) are also plotted in the right side of Fig. 4. The obtained graph has a sigmoidal shape. This sigmoidal shape resembles to a simple logistic function. The sigmoidal relation between the absorption and pH is carefully examined and a useful correlation is produced. As a result, the following equation (Eq. 1) is derived. According to this equation all absorption values for the pHs used are calculated and the obtained corrected sigmoidal curve is given in Fig. 5a. According to Fig. 5a the absorption values obtained by experimental measurements (see Fig. 5a-1) are very close to those obtained by calculation using the Eq. 1.

$$A_{440} = \frac{3}{2 * [1 + 6^{(7-pH)}]} \quad (1)$$

Scheme 2 Protonation-deprotonation equilibria of HBANP

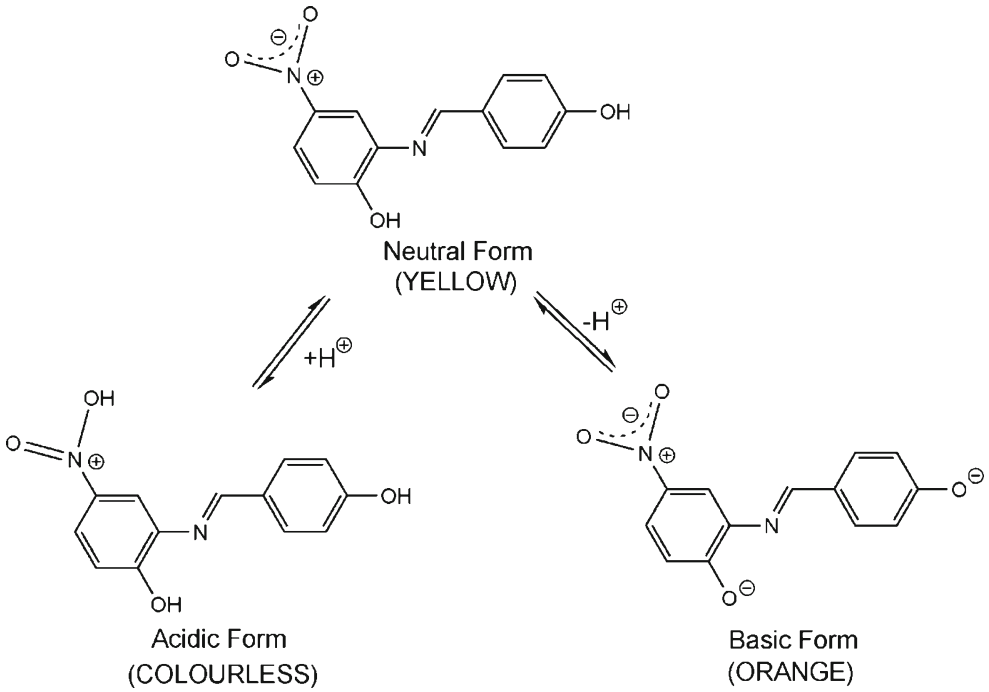

The absorption spectra of PHBANP are also normalized in the range of 250–300 nm and given in Fig. 6. Similarly, absorption increases are obtained for 341 and 409 nm with increasing pH. The spectral responses of PHBANP to the solution pH are plotted in Fig. 6 as the absorption intensities at 409 nm. As seen in Fig. 6, the absorption change at 409 nm starts at pH=3 which shows a linear response between pH=3–5, sharply increases between pH:5–6 and then tends to level off. The absorption change of PHBANP at 409 nm also indicates S-like shape. A similar curve could be obtained by Eq. 2 (Fig. 5b). The corrected curve looks like the obtained from the experimental results. However, especially at high pHs some deviations from the real curve are observed.

$$A_{409} = 0.25 + \frac{5}{4 * \left[1 + 2.5^{(6-pH)}\right]} \quad (2)$$

On the other hand, as seen in the correlations of peak absorptions vs. pHs, linearly responses to pH change are limited in specific pH ranges. For example, HBANP has a

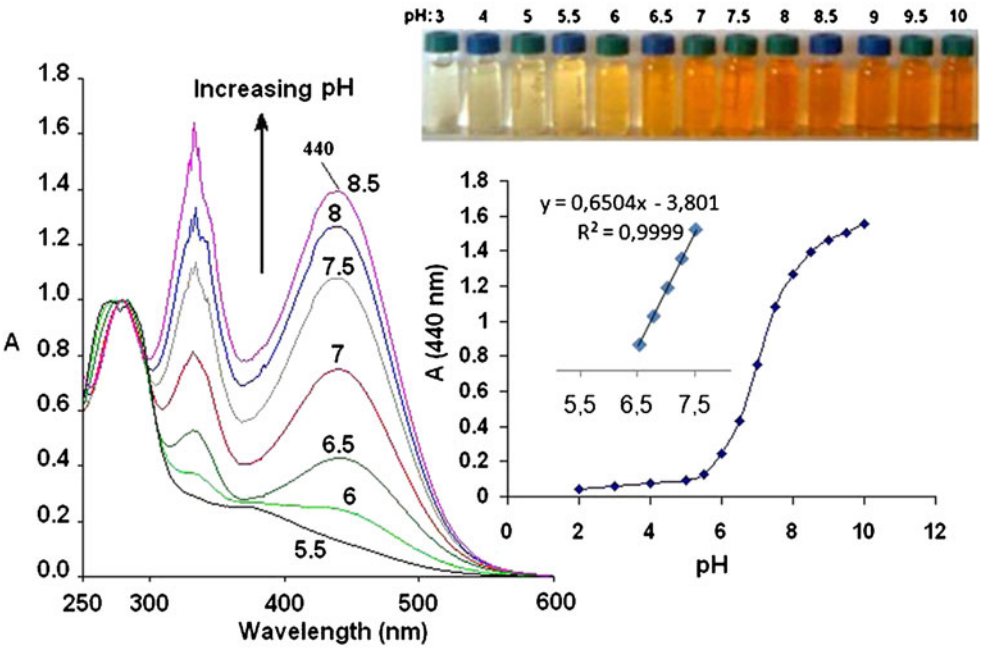

Fig. 4 Spectrophotometric response of HBANP to various pHs, insert; plotted absorbance data at 440 nm vs. pH, top photograph; the colour changes of HBANP solution at different pHs. Conc. of HBANP: 5×10^{-5} kg L^{-1}

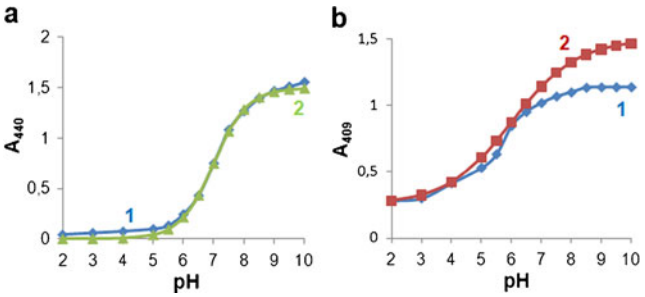

Fig. 5 Sigmoidal correlation of the peak absorbances vs. pHs (1) and the corrected sigmoidal curves according to the related equations (2) for HBANP (**a**) and PHBANP (**b**) solutions

linear response in the range of pH=6.5–7.5 (see Fig. 4). The regression coefficient of HBANP at that pH range is 0.9999. The following equation (Eq. 3) derived from the spectral response of HBANP in the range of pH =6.5–7.5 could be used in pH measurements:

$$\mathrm{pH} = \frac{\mathrm{A}(440) + 3.801}{0.6504} \tag{3}$$

where A(440) is the absorbance of the tested sample at 440 nm.

Similarly, a linear response is obtained by PHBANP solutions in the pH range of 3–5 whose regression coefficient is 0.9961. This means that, PHBANP could be more efficiently used as a new pH sensor in this acidic pH range. The following equation (Eq. 4) is derived from the linear response in the pH range of 3–5 depending on six separate measurements:

$$\mathrm{pH} = \frac{\mathrm{A}(409) + 0.0087}{0.101} \tag{4}$$

where A(409) is the absorbance of the tested sample at 409 nm.

It's seen that PHBANP spectrophotometrically responds to pH change in lower pHs compared to its monomer compound (HBANP). The absorption change of PHBANP becomes very low at the pHs in which the absorption intensity of HBANP particularly increases. This opposite tendency of HBANP and PHBANP could be explained by deprotonation mechanism in basic conditions (see Scheme 2). As emphasized above, in basic conditions the synthesized phenolic compounds transform to phenoxy anion forms by deprotonation. However, the very low spectral change of PHBANP in the basic pHs is attributed to the absence or low number of -OH groups in the polymer chain which results in lower acidity of the polymer. This may be result of the high number of C-O-C coupling of the monomer units during the OP, as mentioned above. The coupling mechanisms of phenolic compounds had been previously studied and two possible mechanisms were suggested: The first is the C-C coupling of the aromatic rings and the second one is the C-O-C coupling that causes a decrease in the -OH numbers. As a result, PHBANP could be used as the alternative pH sensor in the acidic conditions (pH:3–5) while HBANP could be used in the neutral pHs (pH: 6.5–7.5) due to their linear responses and relatively high absorption increases. According to the obtained results the relative spectrophotometric responses (Rr) of the synthesized compounds are determined by using the following equation (Eq. 5) and shown in Fig. 7.

$$\mathrm{Rr} = \frac{\mathrm{A(x)} - \mathrm{A(min)}}{\mathrm{A(max)} - \mathrm{A(min)}} \tag{5}$$

where A(x) is absorbance of the employed spectrum, A(min) and A(max) are the minimum and maximum absorbances, respectively, obtained at the peak wavelengths.

Fluorescence Characteristics

Different Schiff base compounds have been previously studied as emission/excitation based pH probes [36]. Emission and excitation based spectral characteristics of HBANP are determined in the pH range of 4.0–10.0. The signal changes of emission-excitation spectra of HBANP are also monitored at different pHs as shown in Fig. 8. HBANP exhibits

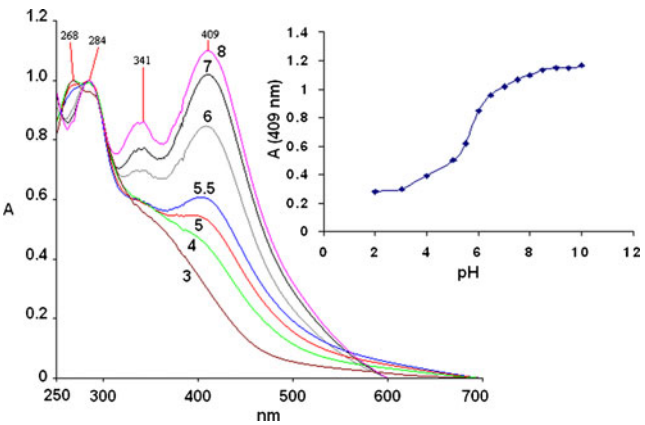

Fig. 6 Spectrophotometric response of PHBANP to various pHs, insert; plotted absorbance data at 409 nm vs. pH. Conc. of PHBANP: 5×10^{-5} kg L^{-1}

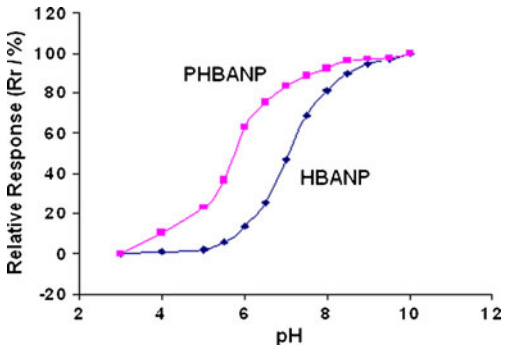

Fig. 7 Relative spectrophotometric response (Rr) of HBANP and PHBANP in the pH range of 3–10. Conc. of HBANP/PHBANP: 5×10^{-5} kg L^{-1}

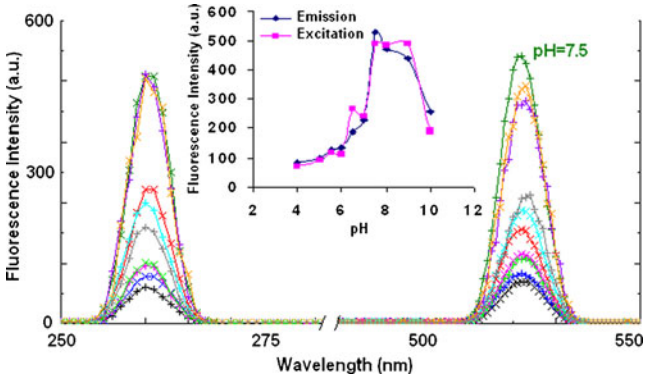

Fig. 8 Fluorescence spectra of HBANP at various pH values, insert; the changes of emission intensities at 523 nm and excitation intensities at 260 nm (λ_{Ex} 268 nm, λ_{Em} 300 nm, Slit: λ_{Ex} 5 nm, λ_{Em} 5 nm). Conc. of HBANP: 5×10^{-5} kg L^{-1}

a clear yellowish emission with an emission maximum at 523 nm. HBANP exhibits an increasing fluorescence signal up to pH: 7.5, reaches to a maximum intensity at this pH, and then sharply decreases with increasing pH. 84% and 86% relative signal changes in direction of decrease in emission and excitation intensities between pH 4.0–7.5 are observed. However, fluorescence based spectral changes of HBANP could not be useful in pH sensor applications due to its irregular intensity changes.

Electrochemical Responses

The electrochemical oxidation behaviours of HBANP related to the solution pH and scan rate were investigated. The cyclic voltammetry (CV) technique was employed with one segment in all measurements. The scan rate (SR) dependence of the oxidation of HBANP in the range of 25–1,000 mV/s is shown in Fig. 9a. As seen in Fig. 9a the oxidation peak current (i_p) particularly increases with increasing SR. The obtained i_p values at the potential of 242 mV are also plotted in Fig. 9b. A linear change is obtained with R=0.986, as indicates the following relationship: $i_p(A) = 3 \times 10^{-8}SR + 6 \times 10^{-6}$.

The pH dependence of the oxidation of HBANP is given in Fig. 10. Figure 10a shows the CVs of HBANP at a few pHs chosen. At the first glance into these CVs it is seen that the peak potential decreases with increasing pH. Figure 10b shows the plotted peak potentials (*Ep*) vs. pHs indicating a sharp *Ep* decrease up to pH:6 and a low decrease between 6 and 9 following by an increase above pH:9. According to the structural forms in different conditions (see Scheme 2) HBANP loses the phenolic protons at the high pHs and the obtained phenoxy anion form facilitates the oxidation of HBANP to form phenoxy radicals. As a result, a lower potential is needed to oxidize HBANP in higher pHs. On the other hand, the relationship between the i_p and pH

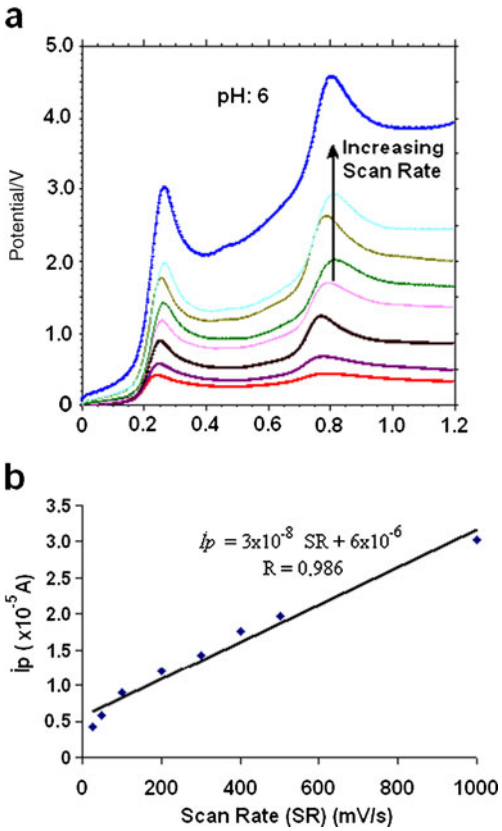

Fig. 9 **a** Cyclic voltammograms of 1 gL^{-1} concentrated HBANP at GCE, scan rates (from bottom to top): 25, 50, 100, 200, 300, 400, 500, and 1,000 mV/s. **b** Linear plotted peak currents of HBANP vs. different scan rates

(shown in Fig. 10c) is in accordance with the results obtained as optically: In the range of pH=6–8 a considerable i_p decrease is obtained. This means that HBANP electrochemically responds in that pH range as decreasing peak current. As mentioned above, HBANP optically responds in the same pH range.

The pH dependence of the oxidation of PHBANP are also given in Fig. 11. As seen in Fig. 11a and b, like HBANP, the oxidation peak potential of PHBANP decreases with increasing pH until pH:7. Above this pH Ep changes only a little. In addition, the changes in the peak currents are irregular (Fig. 11c), thus, it is too hard to explain the pH effect on the i_p of PHBANP.

Conclusion

A new Schiff base and its polyphenol derivative (HBANP and PHBANP) were synthesized and investigated as alternative pH sensors. Structural characterization was made by FT-IR, NMR, and GPC techniques. Spectrophotometric and spectrofluorometric behaviors of the synthesized compounds were studied in different pH values in the range of pH=3–10. The

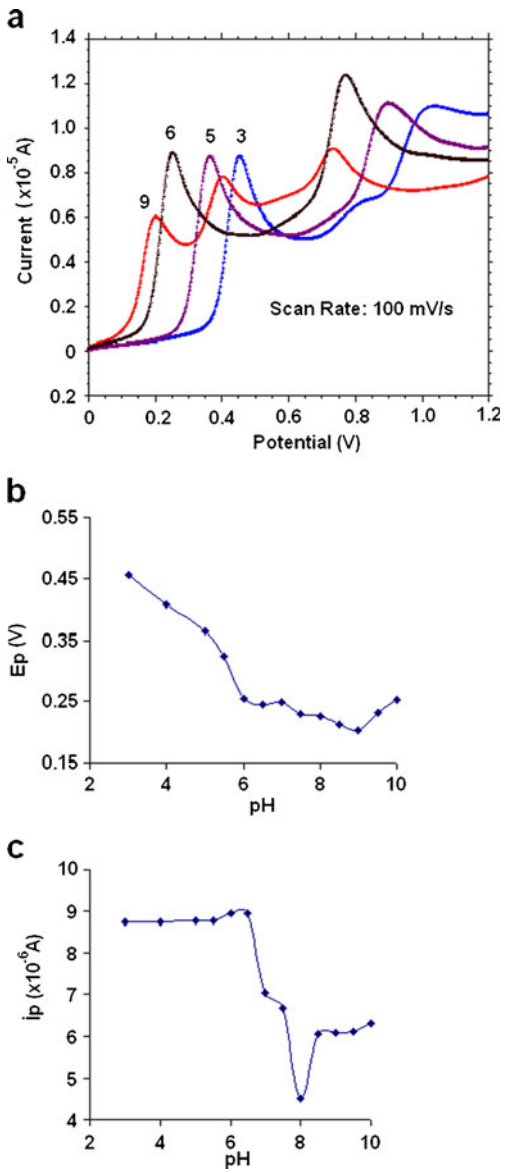

Fig. 10 **a** Cyclic voltammograms of 1 gL^{-1} concentrated HBANP at GCE at various pHs, **b** the relationship of peak potentials vs. pH, and **c** the relationship of peak currents vs. pH

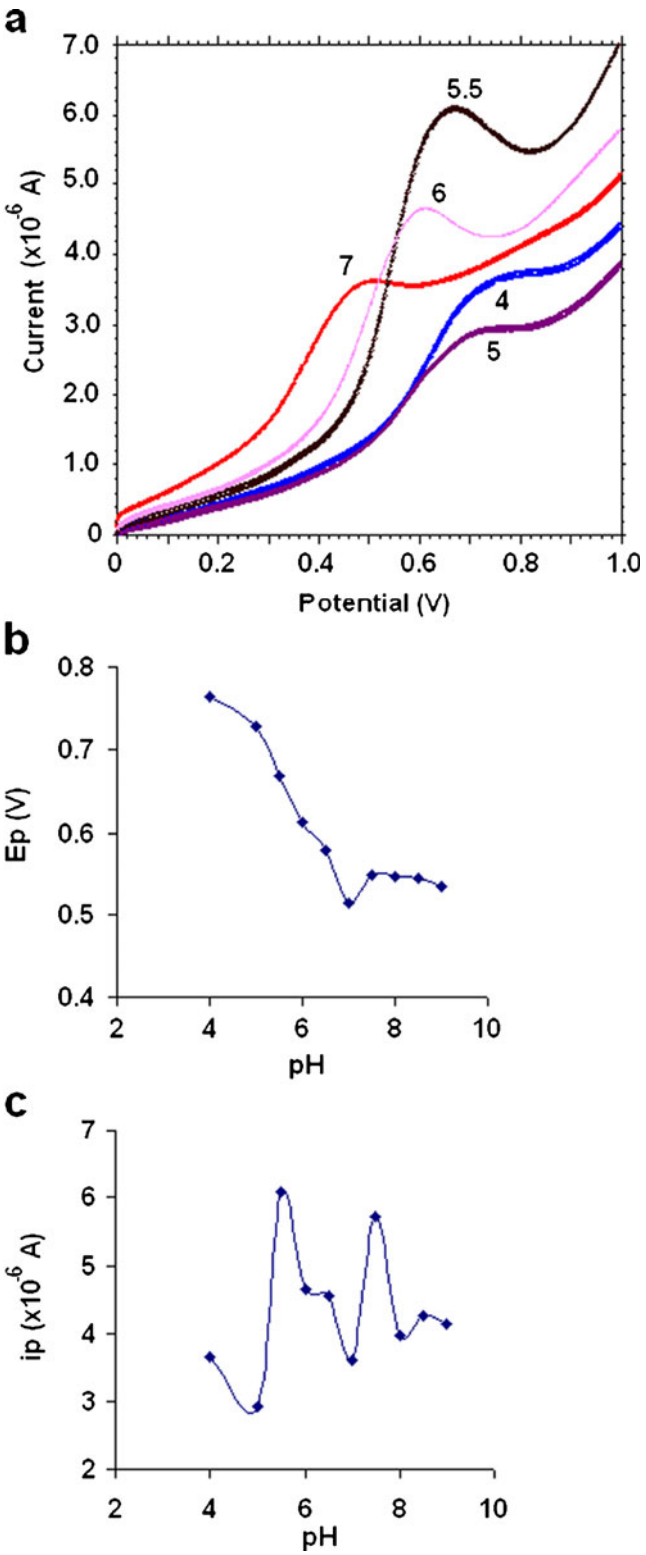

Fig. 11 **a** Cyclic voltammograms of 1 gL^{-1} concentrated PHBANP at GCE at various pHs, **b** the relationship of peak potentials vs. pH, and **c** the relationship of peak currents vs. pH

obtained results showed that the synthesized compounds had a considerable response to solution pH. However, the response range of HBANP and PHBANP were different; HBANP had a sensitive linear response in the range of pH=6.5–7.5 while PHBANP responds to pH change in acidic conditions whose linear change is limited in the range of pH=3–5. PHBANP was found to have lower acidity than its monomer compound because of the C-O-C coupling which decreases the phenolic -OH numbers. Resultantly, we demonstrate that due to their available active centers for proton attacks the novel Schiff base and its polyphenol derivative can be used as alternative spectrophotometric pH sensors for different pH ranges. HBANP can be also used as color-tunable pH sensor in practice. Fluorescence characteristics of HBANP were investigated in different pHs. HBANP showed clear changes in

fluorescence intensities depending on various pHs. Electrochemical oxidation potentials and the peak currents of HBANP and PHBANP also changed considerably related to pH change. As a result, being producted easily and inexpensively, HBANP and PHBANP could be alternative pH probes by using optical or electrochemical techniques.

References

1. Janata J, Bezegh A (1988) Chemical sensors. Anal Chem 60:62R–74R
2. Lee SH, Kumar J, Tripathy SK (2000) Thin film optical sensors employing polyelectrolyte assembly. Langmuir 16:10482–10489
3. Dilek G, Akkaya EU (2000) Novel squaraine signalling Zn(II) ions: three-state fluorescence response to a single input. Tetrahedron Lett 41:3721–3724
4. Demirel A, Dogan A, Canel E, Memon S, Yılmaz M, Kılıç E (2004) Hydrogen ion-selective poly(vinyl chloride) membrane electrode based on a *p*-tert-butylcalix[4]arene-oxacrown-4. Talanta 62:123–129
5. Kriksunov LB, Macdonald DD (1994) Development of glass pH sensors for use at temperatures of 200–250-degrees-C. Sensor Actuat B-Chem 22:201–204
6. Peterson JI, Goldstein SR, Fitzgerald RV, Buckhold DK (1980) Fiber optic pH probe for physiological use. Anal Chem 52:864–869
7. Kirkbright GF, Narayanaswamy R, Welti NA (1984) Fibre-optic pH probe based on the use of an immobilized colorimetric indicator. Analyst 109:1025–1028
8. Misra V, Mishra H, Joshi HC, Pant TC (2002) An optical pH sensor based on excitation energy transfer in Nafion (R) film. Sensor Actuat B-Chem 82:133–141
9. Li ZZ, Niu CG, Zeng GM, Liu YG, Gao PF, Huang GH, Mao YA (2006) A novel fluorescence ratiometric pH sensor based on covalently immobilized piperazinyl-1,8-napthalimide and benzothioxanthene. Sensor Actuat B-Chem 114:308–315
10. Aksuner N, Henden E, Yilmaz I, Cukurovali A (2010) Development of a highly sensitive and selective optical chemical sensor for the determination of zinc based on fluorescence quenching of a novel Schiff base ligand. Sensor Lett 8:684–689
11. Munkholm C, Walt DR, Milanovich FP, Clainer SM (1986) Polymer modification of fiber optic chemical sensors as a method of enhancing fluorescence signal for pH measurement. Anal Chem 58:1427–1430
12. Kostov Y, Tzonkov S, Yotova L, Krysteva M (1993) Membranes for optical pH sensors. Anal Chim Acta 280:15–19
13. Rouhani S, Salimi S, Haghbeen K (2008) Development of optical pH sensors based on derivatives of hydroxyazobenzene, and the extended linear dynamic range using mixture of dyes. Dyes Pigments 77:363–368
14. Safavi A, Abdollahi H (1998) Optical sensor for high pH values. Anal Chim Acta 367:167–173
15. Young VG, Quiring HL, Sykes AG (1997) A luminescent sensor responsive to common oxoacids: X-ray crystal structure of [H3O center dot 1,8-oxybis(ethyleneoxyethyleneoxy) anthracene-9,10-dione]ClO4. J Am Chem Soc 119:12477–12480
16. Safavi A, Bagheri M (2003) Novel optical pH sensor for high and low pH values. Sens Sensors and Actuators B-Chemical Sensor Actuat B-Chem 90:143–150
17. Su MH, Liu Y, Ma HM, Ma QL, Wang ZH, Yang JL, Wang MX (2001) 1,9-Dihydro-3-phenyl-4H-pyrazolo[3,4-b]quinolin-4-one, a novel fluorescent probe for extreme pH measurement. Chem Commun 11:960–961
18. Gunnlaugsson T (2001) A novel Eu(III)-based luminescent chemosensor: determining pH in a highly acidic environment. Tetrahedron Lett 42:8901–8905
19. Nishimura G, Shiraishi Y, Hirai T (2005) A fluorescent chemosensor for wide-range pH detection. Chem Commun 42:5313–5315
20. Jin Z, Su YX, Duan YX (2000) An improved optical pH sensor based on polyaniline. Sensor Actuat B-Chem 71:118–122
21. Yue F, Ngin TS, Hailin G (1996) A novel paper pH sensor based on polypyrrole. Sensor Actuat B-Chem 32:33–39
22. Trinh QT, Gerlach G, Sorber J, Arndt KF (2006) Hydrogel-based piezoresistive pH sensors: design, simulation and output characteristics. Sensor Actuat B-Chem 117:17–26
23. Gerlach G, Guenther M, Sorber J, Suchaneck G, Arndt KF, Richter A (2005) Chemical and pH sensors based on the swelling behavior of hydrogels. Sensor Actuat B-Chem 111:555–561
24. Bazzicalupi C, Bencini A, Biagini S, Faggi E, Farruggia G, Andreani G, Gratteri P, Prodi L, Spepia A, Valtancolia B (2010) A highly pH-sensitive Zn(II) chemosensor. Dalton T 39:7080–7090
25. Fotouhi L, Hajilari F, Heravi MM (2002) Lectrochemical behavior of some thiotriazoles in aqueous-alcoholic media at GCE. Electroanal 14:1728–1732
26. Kaya İ, Bilici A (2007) Synthesis, characterization, thermal analysis, and band gap of oligo-2-methoxy-6-[(4-methylphenyl)imino] methylphenol. J Appl Polym Sci 104:3417–3426
27. Kaya İ, Bilici A (2007) Syntheses, structures, electric conduction, electrochemical properties and antimicrobial activity of azomethine monomer and oligomer based on 4-hydroxybenzaldehyde and 2-aminopyridine. Polimery 52:827–835
28. Kaya İ, Yıldırım M, Kamacı M (2009) Synthesis and characterization of new polyphenols derived from o-dianisidine: the effect of substituent on solubility, thermal stability, and electrical conductivity, optical and electrochemical properties. Eur Polym J 45:1586–1598
29. Ikeda R, Sugihara J, Uyama H, Kobayashi S (1996) Enzymatic oxidative polymerization of 2,6-dimethylphenol. Macromolecules 29:8702–8705
30. Kaya İ, Bilici A, Yıldırım M, Dogan F (2010) Enzymatic polymerization of hydroxy-functionalized carbazole monomer. J Mol Catal B Enzym 64:89–95
31. Yadav BS, Ali I, Kumar P, Yadav P (2007) FTIR and laser Raman spectra of 2-hydroxy-5-methyl-3-nitro pyridine. Indian J Pure Appl Phys 45:979–983
32. Kaya İ, Yıldırım M, Aydın A, Şenol D (2010) Synthesis and characterization of fluorescent graft fluorene-co-polyphenol derivatives: the effect of substituent on solubility, thermal stability, conductivity, optical and electrochemical properties. React Funct Polym 70:815–826
33. Zheng GR, Wang ZX, Tang L, Lu P, Weber WP (2007) Color tunable, ratiometric pH sensor for high and low pH values base on 9-(cycloheptatrienylidene)fluorene derivatives. Sensor Actuat B-Chem 122:389–394
34. Bissell RA, deSilva AP, Gunaratne HQN, Lynch PLM, Maguire GEM, McCoy CP, Sandanayake KRAS (1993) Fluorescent PET (photoinduced electron-transfer) sensors. Top Curr Chem 168:223–264
35. Saravanakumar D, Devaraj S, Iyyampillai S, Mohandoss K, Kandaswamy M (2008) Schiff's base phenol-hydrazone derivatives as colorimetric chemosensors for fluoride ions. Tetrahedron Lett 49:127–132
36. Derinkuyu S, Ertekin K, Oter O, Denizalti S, Cetinkaya E (2007) Fiber optic pH sensing with long wavelength excitable Schiff bases in the pH range of 7.0–12.0. Anal Chim Acta 588:42–49